E-ISSN: 2708-4485
P-ISSN: 2708-4477
IJEDN 2022; 3(1): 12-22
© 2022 IJEDN
www.electronicnetjournal.com
Received: 07-10-2021
Accepted: 09-12-2021

EL Pankratov
[1] Nizhny Novgorod State University, 23 Gagarin Avenue, Nizhny Novgorod, 603950, Russia
[2] Nizhny Novgorod State Technical University, 24 Minin Street, Nizhny Novgorod, 603950, Russia

Correspondence Author;
EL Pankratov
[1] Nizhny Novgorod State University, 23 Gagarin Avenue, Nizhny Novgorod, 603950, Russia
[2] Nizhny Novgorod State Technical University, 24 Minin Street, Nizhny Novgorod, 603950, Russia

On increasing of density of field-effect heterotransistors in the framework of a C-multiplier. Influence of mismatch-induced stress and porosity of materials on technological process

EL Pankratov

Abstract
In this paper we introduce an analytical approach to analyze mass and heat transport in heterostructures during manufacturing of integrated circuits with account mismatch-induced stress. Based on this approach we analyzed possibility to increase density of field-effect transistors framework a *C*-multiplier. Framework the approach we consider manufacturing the inverter in heterostructure with specific configuration. Several required areas of the heterostructure should be doped by diffusion or ion implantation. After that dopant and radiation defects should by annealed framework optimized scheme. We also consider an approach to decrease value of mismatch-induced stress in the considered heterostructure.

Keywords: Analytical approach for modelling, C-multiplier, optimization of manufacturing, accounting of mismatch induced stress and porosity of materials.

Introduction

In the present time several actual problems of the solid state electronics (such as increasing of performance, reliability and density of elements of integrated circuits: diodes, field-effect and bipolar transistors) are intensively solving [1-6]. To increase the performance of these devices it is attracted an interest determination of materials with higher values of charge carrier's mobility [7-10]. One way to decrease dimensions of elements of integrated circuits is manufacturing them in thin film heterostructures [3-5, 11]. In this case it is possible to use inhomogeneity of heterostructure and necessary optimization of doping of electronic materials [12] and development of epitaxial technology to improve these materials (including analysis of mismatch induced stress) [13-15]. An alternative approaches to increase dimensions of integrated circuits are using of laser and microwave types of annealing [16-18].
Framework the paper we introduce an approach to manufacture field-effect transistors. The approach gives a possibility to decrease their dimensions with increasing their density framework a *C*-multiplier. We also consider possibility to decrease mismatch-induced stress to decrease quantity of defects, generated due to the stress. In this paper we consider a heterostructure, which consist of a substrate and an epitaxial layer (see Fig. 1). We also consider a buffer layer between the substrate and the epitaxial layer. The epitaxial layer includes into itself several sections, which were manufactured by using another materials. These sections have been doped by diffusion or ion implantation to manufacture the required types of conductivity (*p* or *n*). These areas became sources, drains and gates (see Fig. 1). After this doping it is required annealing of dopant and/or radiation defects. Main aim of the present paper is analysis of redistribution of dopant and radiation defects to determine conditions, which correspond to decreasing of elements of the considered *C*-multiplier and at the same time to increase their density. At the same time we consider a possibility to decrease mismatch-induced stress.

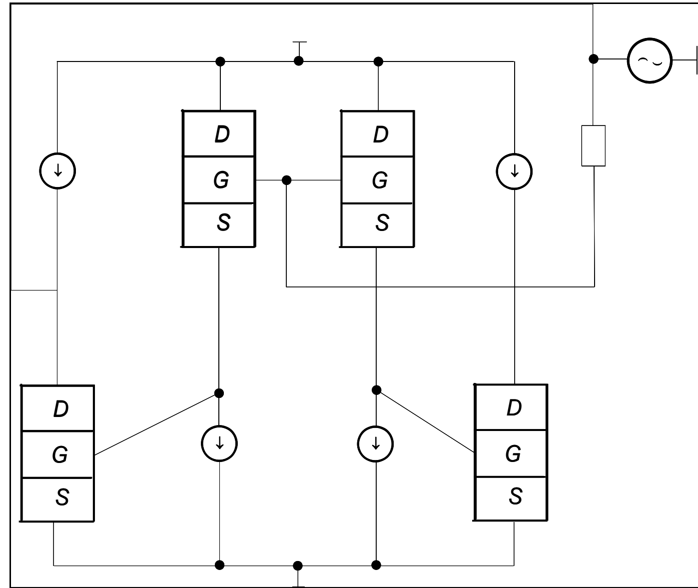

Fig 1a: Structure of the considered *C*-multiplier [19]

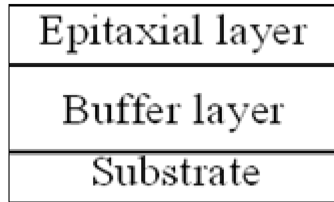

Fig 1b: Heterostructure with a substrate, epitaxial layers and buffer layer (view from side)

Mathematical model

To solve our aim we determine and analyzed spatio-temporal distribution of concentration of dopant in the considered heterostructure. We determine the distribution by solving the second Fick's law in the following form [1, 20-23]

$$\frac{\partial C(x,y,z,t)}{\partial t}=\frac{\partial}{\partial x}\left[D\frac{\partial C(x,y,z,t)}{\partial x}\right]+\frac{\partial}{\partial y}\left[D\frac{\partial C(x,y,z,t)}{\partial y}\right]+\frac{\partial}{\partial z}\left[D\frac{\partial C(x,y,z,t)}{\partial z}\right]+$$
$$+\Omega\frac{\partial}{\partial x}\left[\frac{D_S}{kT}\nabla_S\mu_1(x,y,z,t)\int_0^{L_z}C(x,y,W,t)dW\right]+$$
$$+\Omega\frac{\partial}{\partial y}\left[\frac{D_S}{kT}\nabla_S\mu_1(x,y,z,t)\int_0^{L_z}C(x,y,W,t)dW\right]+ \tag{1}$$
$$+\frac{\partial}{\partial x}\left[\frac{D_{CS}}{\bar{V}kT}\frac{\partial\mu_2(x,y,z,t)}{\partial x}\right]+\frac{\partial}{\partial y}\left[\frac{D_{CS}}{\bar{V}kT}\frac{\partial\mu_2(x,y,z,t)}{\partial y}\right]+\frac{\partial}{\partial z}\left[\frac{D_{CS}}{\bar{V}kT}\frac{\partial\mu_2(x,y,z,t)}{\partial z}\right]$$

With boundary and initial conditions

$$\left.\frac{\partial C(x,y,z,t)}{\partial x}\right|_{x=0}=0,\ \left.\frac{\partial C(x,y,z,t)}{\partial x}\right|_{x=L_x}=0,\ \left.\frac{\partial C(x,y,z,t)}{\partial y}\right|_{y=0}=0,\ C(x,y,z,0)=f_C(x,y,z),$$
$$\left.\frac{\partial C(x,y,z,t)}{\partial y}\right|_{x=L_y}=0,\ \left.\frac{\partial C(x,y,z,t)}{\partial z}\right|_{z=0}=0,\ \left.\frac{\partial C(x,y,z,t)}{\partial z}\right|_{x=L_z}=0.$$

Here $C(x, y, z, t)$ is the spatio-temporal distribution of concentration of dopant; Ω is the atomic volume of dopant; ∇_s is the symbol of surficial gradient; $\int_0^{L_z} C(x,y,z,t)\,d\,z$ is the surficial concentration of dopant on interface between layers of heterostructure (in this situation we assume, that Z-axis is perpendicular to interface between layers of heterostructure); $\mu_1(x, y, z, t)$ and $\mu_2(x, y, z, t)$ are the chemical potential due to the presence of mismatch-induced stress and porosity of material; D and D_S are the coefficients of volumetric and surficial diffusions. Values of dopant diffusions coefficients depends on properties of materials of heterostructure, speed of heating and cooling of materials during annealing and spatio-temporal distribution of concentration of dopant. Dependences of dopant diffusions coefficients on parameters could be approximated by the following relations [24-26].

$$D_C = D_L(x,y,z,T)\left[1+\xi\frac{C^\gamma(x,y,z,t)}{P^\gamma(x,y,z,T)}\right]\left[1+\varsigma_1\frac{V(x,y,z,t)}{V^*}+\varsigma_2\frac{V^2(x,y,z,t)}{(V^*)^2}\right],$$

$$D_S = D_{SL}(x,y,z,T)\left[1+\xi_S\frac{C^\gamma(x,y,z,t)}{P^\gamma(x,y,z,T)}\right]\left[1+\varsigma_1\frac{V(x,y,z,t)}{V^*}+\varsigma_2\frac{V^2(x,y,z,t)}{(V^*)^2}\right]. \quad (2)$$

Here $D_L(x, y, z, T)$ and $D_{LS}(x, y, z, T)$ are the spatial (due to accounting all layers of heterostruicture) and temperature (due to Arrhenius law) dependences of dopant diffusion coefficients; T is the temperature of annealing; $P(x, y, z, T)$ is the limit of solubility of dopant; parameter γ depends on properties of materials and could be integer in the following interval $\gamma\in$ [1, 3, 24] $V(x, y, z, t)$ is the spatio-temporal distribution of concentration of radiation vacancies; V^* is the equilibrium distribution of vacancies. Concentration dependence of dopant diffusion coefficient has been described in details in [24]. Spatio-temporal distributions of concentration of point radiation defects have been determined by solving the following system of equations [20-23, 25, 26].

$$\frac{\partial I(x,y,z,t)}{\partial t}=\frac{\partial}{\partial x}\left[D_I(x,y,z,T)\frac{\partial I(x,y,z,t)}{\partial x}\right]+\frac{\partial}{\partial y}\left[D_I(x,y,z,T)\frac{\partial I(x,y,z,t)}{\partial y}\right]+$$
$$+\frac{\partial}{\partial z}\left[D_I(x,y,z,T)\frac{\partial I(x,y,z,t)}{\partial z}\right]-k_{I,I}(x,y,z,T)\,I^2(x,y,z,t)-k_{I,V}(x,y,z,T)\times$$
$$\times I(x,y,z,t)V(x,y,z,t)+\Omega\frac{\partial}{\partial x}\left[\frac{D_{IS}}{kT}\nabla_S\mu\,(x,y,z,t)\int_0^{L_z}I(x,y,W,t)\,d\,W\right]+$$
$$+\Omega\frac{\partial}{\partial y}\left[\frac{D_{IS}}{kT}\nabla_S\mu\,(x,y,z,t)\int_0^{L_z}I(x,y,W,t)\,d\,W\right]+\frac{\partial}{\partial x}\left[\frac{D_{IS}}{\bar V kT}\frac{\partial\mu_2(x,y,z,t)}{\partial x}\right]+$$
$$+\frac{\partial}{\partial y}\left[\frac{D_{IS}}{\bar V kT}\frac{\partial\mu_2(x,y,z,t)}{\partial y}\right]+\frac{\partial}{\partial z}\left[\frac{D_{IS}}{\bar V kT}\frac{\partial\mu_2(x,y,z,t)}{\partial z}\right] \quad (3)$$

$$\frac{\partial V(x,y,z,t)}{\partial t}=\frac{\partial}{\partial x}\left[D_V(x,y,z,T)\frac{\partial V(x,y,z,t)}{\partial x}\right]+\frac{\partial}{\partial y}\left[D_V(x,y,z,T)\frac{\partial V(x,y,z,t)}{\partial y}\right]+$$
$$+\frac{\partial}{\partial z}\left[D_V(x,y,z,T)\frac{\partial V(x,y,z,t)}{\partial z}\right]-k_{V,V}(x,y,z,T)\,V^2(x,y,z,t)-k_{I,V}(x,y,z,T)\times$$

$$\times I(x,y,z,t)V(x,y,z,t)+\Omega\frac{\partial}{\partial x}\left[\frac{D_{VS}}{kT}\nabla_S\mu(x,y,z,t)\int_0^{L_z}V(x,y,W,t)\,dW\right]+$$

$$+\Omega\frac{\partial}{\partial y}\left[\frac{D_{VS}}{kT}\nabla_S\mu(x,y,z,t)\int_0^{L_z}V(x,y,W,t)dW\right]+\frac{\partial}{\partial x}\left[\frac{D_{VS}}{\bar{V}kT}\frac{\partial\mu_2(x,y,z,t)}{\partial x}\right]+$$

$$+\frac{\partial}{\partial y}\left[\frac{D_{VS}}{\bar{V}kT}\frac{\partial\mu_2(x,y,z,t)}{\partial y}\right]+\frac{\partial}{\partial z}\left[\frac{D_{VS}}{\bar{V}kT}\frac{\partial\mu_2(x,y,z,t)}{\partial z}\right]$$

With boundary and initial conditions

$$\left.\frac{\partial I(x,y,z,t)}{\partial x}\right|_{x=0}=0,\ \left.\frac{\partial I(x,y,z,t)}{\partial x}\right|_{x=L_x}=0,\ \left.\frac{\partial I(x,y,z,t)}{\partial y}\right|_{y=0}=0,$$

$$\left.\frac{\partial I(x,y,z,t)}{\partial y}\right|_{y=L_y}=0,\ \left.\frac{\partial I(x,y,z,t)}{\partial z}\right|_{z=0}=0,\ \left.\frac{\partial I(x,y,z,t)}{\partial z}\right|_{z=L_z}=0,$$

$$\left.\frac{\partial V(x,y,z,t)}{\partial x}\right|_{x=0}=0\ \left.\frac{\partial V(x,y,z,t)}{\partial x}\right|_{x=L_x}=0,\ \left.\frac{\partial V(x,y,z,t)}{\partial y}\right|_{y=0}=0\ (4)$$

$$\left.\frac{\partial V(x,y,z,t)}{\partial y}\right|_{y=L_y}=0,\ \left.\frac{\partial V(x,y,z,t)}{\partial z}\right|_{z=0}=0,\ \left.\frac{\partial V(x,y,z,t)}{\partial z}\right|_{z=L_z}=0,\ I(x,y,z,0)=$$

$$=f_I(x,y,z),\ V(x,y,z,0)=f_V(x,y,z),\ V(x_1+V_nt,y_1+V_nt,z_1+V_nt,t)=V_\infty\left(1+\frac{2\ell\omega}{kT\sqrt{x_1^2+y_1^2+z_1^2}}\right).$$

Here $I(x, y, z, t)$ is the spatio-temporal distribution of concentration of radiation interstitials; I^* is the equilibrium distribution of interstitials; $D_I(x, y, z, T)$, $D_V(x, y, z, T)$, $D_{IS}(x, y, z, T)$, $D_{VS}(x, y, z, T)$ are the coefficients of volumetric and surficial diffusions of interstitials and vacancies, respectively; terms $V^2(x, y, z, t)$ and $I^2(x, y, z, t)$ correspond to generation of divacancies and diinterstitials, respectively (see, for example, [26] and appropriate references in this book); $k_{I,V}(x, y, z, T)$, $k_{I,I}(x, y, z, T)$ and $k_{V,V}(x, y, z, T)$ are the parameters of recombination of point radiation defects and generation of their complexes; k is the Boltzmann constant; $\omega = a^3$, a is the interatomic distance; ℓ is the specific surface energy. To account porosity of buffer layers we assume, that porous are approximately cylindrical with average values $r=\sqrt{x_1^2+y_1^2}$ and z_1 before annealing [23]. With time small pores decomposing on vacancies. The vacancies absorbing by larger pores [27]. With time large pores became larger due to absorbing the vacancies and became more spherical [27]. Distribution of concentration of vacancies in heterostructure, existing due to porosity, could be determined by summing on all pores, i.e.

$$V(x,y,z,t)=\sum_{i=0}^{l}\sum_{j=0}^{m}\sum_{k=0}^{n}V_p(x+i\alpha,y+j\beta,z+k\chi,t),\ R=\sqrt{x^2+y^2+z^2}.$$

Here α, β and χ are the average distances between centers of pores in directions x, y and z; l, m and n are the quantity of pores inappropriate directions.
Spatio-temporal distributions of divacancies $\Phi_V(x, y, z, t)$ and dinterstitials $\Phi_I(x, y, z, t)$ could be determined by solving the following system of equations [25, 26].

$$\frac{\partial \Phi_I(x,y,z,t)}{\partial t}=\frac{\partial}{\partial x}\left[D_{\Phi_I}(x,y,z,T)\frac{\partial \Phi_I(x,y,z,t)}{\partial x}\right]+\frac{\partial}{\partial y}\left[D_{\Phi_I}(x,y,z,T)\frac{\partial \Phi_I(x,y,z,t)}{\partial y}\right]+$$

$$+\frac{\partial}{\partial z}\left[D_{\Phi_I}(x,y,z,T)\frac{\partial \Phi_I(x,y,z,t)}{\partial z}\right]+\Omega\frac{\partial}{\partial x}\left[\frac{D_{\Phi_I S}}{kT}\nabla_S \mu_1(x,y,z,t)\int\limits_0^{L_z}\Phi_I(x,y,W,t)dW\right]+$$

$$+\Omega\frac{\partial}{\partial y}\left[\frac{D_{\Phi_I S}}{kT}\nabla_S \mu_1(x,y,z,t)\int\limits_0^{L_z}\Phi_I(x,y,W,t)dW\right]+k_{I,I}(x,y,z,T)I^2(x,y,z,t)+$$

$$+\frac{\partial}{\partial x}\left[\frac{D_{\Phi_I S}}{\bar{V}kT}\frac{\partial \mu_2(x,y,z,t)}{\partial x}\right]+\frac{\partial}{\partial y}\left[\frac{D_{\Phi_I S}}{\bar{V}kT}\frac{\partial \mu_2(x,y,z,t)}{\partial y}\right]+\frac{\partial}{\partial z}\left[\frac{D_{\Phi_I S}}{\bar{V}kT}\frac{\partial \mu_2(x,y,z,t)}{\partial z}\right]+$$

$$+k_I(x,y,z,T)I(x,y,z,t) \quad (5)$$

$$\frac{\partial \Phi_V(x,y,z,t)}{\partial t}=\frac{\partial}{\partial x}\left[D_{\Phi_V}(x,y,z,T)\frac{\partial \Phi_V(x,y,z,t)}{\partial x}\right]+\frac{\partial}{\partial y}\left[D_{\Phi_V}(x,y,z,T)\frac{\partial \Phi_V(x,y,z,t)}{\partial y}\right]+$$

$$+\frac{\partial}{\partial z}\left[D_{\Phi_V}(x,y,z,T)\frac{\partial \Phi_V(x,y,z,t)}{\partial z}\right]+\Omega\frac{\partial}{\partial x}\left[\frac{D_{\Phi_V S}}{kT}\nabla_S \mu_1(x,y,z,t)\int\limits_0^{L_z}\Phi_V(x,y,W,t)dW\right]+$$

$$+\Omega\frac{\partial}{\partial y}\left[\frac{D_{\Phi_V S}}{kT}\nabla_S \mu_1(x,y,z,t)\int\limits_0^{L_z}\Phi_V(x,y,W,t)dW\right]+k_{V,V}(x,y,z,T)V^2(x,y,z,t)+$$

$$+\frac{\partial}{\partial x}\left[\frac{D_{\Phi_V S}}{\bar{V}kT}\frac{\partial \mu_2(x,y,z,t)}{\partial x}\right]+\frac{\partial}{\partial y}\left[\frac{D_{\Phi_V S}}{\bar{V}kT}\frac{\partial \mu_2(x,y,z,t)}{\partial y}\right]+\frac{\partial}{\partial z}\left[\frac{D_{\Phi_V S}}{\bar{V}kT}\frac{\partial \mu_2(x,y,z,t)}{\partial z}\right]+$$

$$+k_V(x,y,z,T)V(x,y,z,t)$$

With boundary and initial conditions

$$\left.\frac{\partial \Phi_I(x,y,z,t)}{\partial x}\right|_{x=0}=0,\ \left.\frac{\partial \Phi_I(x,y,z,t)}{\partial x}\right|_{x=L_x}=0,\ \left.\frac{\partial \Phi_I(x,y,z,t)}{\partial y}\right|_{y=0}=0,$$

$$\left.\frac{\partial \Phi_I(x,y,z,t)}{\partial y}\right|_{y=L_y}=0,\ \left.\frac{\partial \Phi_I(x,y,z,t)}{\partial z}\right|_{z=0}=0,\ \left.\frac{\partial \Phi_I(x,y,z,t)}{\partial z}\right|_{z=L_z}=0,$$

$$\left.\frac{\partial \Phi_V(x,y,z,t)}{\partial x}\right|_{x=0}=0,\ \left.\frac{\partial \Phi_V(x,y,z,t)}{\partial x}\right|_{x=L_x}=0,\ \left.\frac{\partial \Phi_V(x,y,z,t)}{\partial y}\right|_{y=0}=0, \quad (6)$$

$$\left.\frac{\partial \Phi_V(x,y,z,t)}{\partial y}\right|_{y=L_y}=0,\ \left.\frac{\partial \Phi_V(x,y,z,t)}{\partial z}\right|_{z=0}=0,\ \left.\frac{\partial \Phi_V(x,y,z,t)}{\partial z}\right|_{z=L_z}=0,$$

$\Phi_I(x, y, z, 0)=f_{\Phi I}(x, y, z)$, $\Phi_V(x,y,z,0)=f_{\Phi V}(x, y, z)$.

Here $D_{\Phi I}(x, y, z, T)$, $D_{\Phi V}(x, y, z, T)$, $D_{\Phi IS}(x, y, z, T)$ and $D_{\Phi VS}(x, y, z, T)$ are the coefficients of volumetric and surficial diffusions of complexes of radiation defects; $k_I(x, y, z, T)$ and $k_V(x, y, z, T)$ are the parameters of decay of complexes of radiation defects.
Chemical potential μ_1 in Eq. (1) could be determine by the following relation [20].

$$\mu_1=E(z)\Omega\sigma_{ij}\,[u_{ij}(x, y, z, t)+u_{ji}(x, y, z, t)]/2, \qquad (7)$$

where $E(z)$ is the Young modulus, σ_{ij} is the stress tensor; $u_{ij}=\frac{1}{2}\left(\frac{\partial u_i}{\partial x_j}+\frac{\partial u_j}{\partial x_i}\right)$ is the deformation tensor; u_i, u_j are the components $u_x(x, y, z, t)$, $u_y(x, y, z, t)$ and $u_z(x, y, z, t)$ of the displacement vector $\vec{u}(x,y,z,t)$; x_i, x_j are the coordinate x, y, z.
The Eq. (3) could be transform to the following form

$$\mu(x,y,z,t)=\left[\frac{\partial u_i(x,y,z,t)}{\partial x_j}+\frac{\partial u_j(x,y,z,t)}{\partial x_i}\right]\left\{\frac{1}{2}\left[\frac{\partial u_i(x,y,z,t)}{\partial x_j}+\frac{\partial u_j(x,y,z,t)}{\partial x_i}\right]-\right.$$

$$\left.-\varepsilon_0\delta_{ij}+\frac{\sigma(z)\delta_{ij}}{1-2\sigma(z)}\left[\frac{\partial u_k(x,y,z,t)}{\partial x_k}-3\varepsilon_0\right]-K(z)\beta(z)\left[T(x,y,z,t)-T_0\right]\delta_{ij}\right\}\frac{\Omega}{2}E(z),$$

Where σ is Poisson coefficient; $\varepsilon_0=(a_s-a_{EL})/a_{EL}$ is the mismatch parameter; a_s, a_{EL} are lattice distances of the substrate and the epitaxial layer; K is the modulus of uniform compression; β is the coefficient of thermal expansion; T_r is the equilibrium temperature, which coincide (for our case) with room temperature. Components of displacement vector could be obtained by solution of the following equations [21].

$$\begin{cases}\rho(z)\frac{\partial^2 u_x(x,y,z,t)}{\partial t^2}=\frac{\partial\sigma_{xx}(x,y,z,t)}{\partial x}+\frac{\partial\sigma_{xy}(x,y,z,t)}{\partial y}+\frac{\partial\sigma_{xz}(x,y,z,t)}{\partial z}\\ \rho(z)\frac{\partial^2 u_y(x,y,z,t)}{\partial t^2}=\frac{\partial\sigma_{yx}(x,y,z,t)}{\partial x}+\frac{\partial\sigma_{yy}(x,y,z,t)}{\partial y}+\frac{\partial\sigma_{yz}(x,y,z,t)}{\partial z}\\ \rho(z)\frac{\partial^2 u_z(x,y,z,t)}{\partial t^2}=\frac{\partial\sigma_{zx}(x,y,z,t)}{\partial x}+\frac{\partial\sigma_{zy}(x,y,z,t)}{\partial y}+\frac{\partial\sigma_{zz}(x,y,z,t)}{\partial z}\end{cases}$$

Where

$$\sigma_{ij}=\frac{E(z)}{2[1+\sigma(z)]}\left[\frac{\partial u_i(x,y,z,t)}{\partial x_j}+\frac{\partial u_j(x,y,z,t)}{\partial x_i}-\frac{\delta_{ij}}{3}\frac{\partial u_k(x,y,z,t)}{\partial x_k}\right]+K(z)\delta_{ij}\times$$

$$\times\frac{\partial u_k(x,y,z,t)}{\partial x_k}-\beta(z)K(z)\left[T(x,y,z,t)-T_r\right],$$

$\rho(z)$ is the density of materials of heterostructure, δ_{ij} Is the Kronecker symbol. With account the relation for σ_{ij} last system of equation could be written as

$$\rho(z)\frac{\partial^2 u_x(x,y,z,t)}{\partial t^2}=\left\{K(z)+\frac{5E(z)}{6[1+\sigma(z)]}\right\}\frac{\partial^2 u_x(x,y,z,t)}{\partial x^2}+\left\{K(z)-\frac{E(z)}{3[1+\sigma(z)]}\right\}\times$$

$$\times\frac{\partial^2 u_y(x,y,z,t)}{\partial x\partial y}+\frac{E(z)}{2[1+\sigma(z)]}\left[\frac{\partial^2 u_y(x,y,z,t)}{\partial y^2}+\frac{\partial^2 u_z(x,y,z,t)}{\partial z^2}\right]+\left[K(z)+\frac{E(z)}{3[1+\sigma(z)]}\right]\times$$

$$\times\frac{\partial^2 u_z(x,y,z,t)}{\partial x\partial z}-K(z)\beta(z)\frac{\partial T(x,y,z,t)}{\partial x}$$

$$\rho(z)\frac{\partial^2 u_y(x,y,z,t)}{\partial t^2}=\frac{E(z)}{2[1+\sigma(z)]}\left[\frac{\partial^2 u_y(x,y,z,t)}{\partial x^2}+\frac{\partial^2 u_x(x,y,z,t)}{\partial x\partial y}\right]-\frac{\partial T(x,y,z,t)}{\partial y}\times$$

$$\times K(z)\beta(z)+\frac{\partial}{\partial z}\left\{\frac{E(z)}{2[1+\sigma(z)]}\left[\frac{\partial u_y(x,y,z,t)}{\partial z}+\frac{\partial u_z(x,y,z,t)}{\partial y}\right]\right\}+\frac{\partial^2 u_y(x,y,z,t)}{\partial y^2}\times \quad (8)$$

$$\times\left\{\frac{5E(z)}{12[1+\sigma(z)]}+K(z)\right\}+\left\{K(z)-\frac{E(z)}{6[1+\sigma(z)]}\right\}\frac{\partial^2 u_y(x,y,z,t)}{\partial y\partial z}+K(z)\frac{\partial^2 u_y(x,y,z,t)}{\partial x\partial y}$$

$$\rho(z)\frac{\partial^2 u_z(x,y,z,t)}{\partial t^2}=\frac{E(z)}{2[1+\sigma(z)]}\left[\frac{\partial^2 u_z(x,y,z,t)}{\partial x^2}+\frac{\partial^2 u_z(x,y,z,t)}{\partial y^2}+\frac{\partial^2 u_x(x,y,z,t)}{\partial x\partial z}+\right.$$

$$\left.+\frac{\partial^2 u_y(x,y,z,t)}{\partial y\partial z}\right]+\frac{\partial}{\partial z}\left\{K(z)\left[\frac{\partial u_x(x,y,z,t)}{\partial x}+\frac{\partial u_y(x,y,z,t)}{\partial y}+\frac{\partial u_x(x,y,z,t)}{\partial z}\right]\right\}+$$

$$+\frac{1}{6}\frac{\partial}{\partial z}\left\{\frac{E(z)}{1+\sigma(z)}\left[6\frac{\partial u_z(x,y,z,t)}{\partial z}-\frac{\partial u_x(x,y,z,t)}{\partial x}-\frac{\partial u_y(x,y,z,t)}{\partial y}-\frac{\partial u_z(x,y,z,t)}{\partial z}\right]\right\}-$$

$$-K(z)\beta(z)\frac{\partial T(x,y,z,t)}{\partial z}.$$

Conditions for the system of Eq. (8) could be written in the form

$$\frac{\partial \vec{u}(0,y,z,t)}{\partial x}=0;\ \frac{\partial \vec{u}(L_x,y,z,t)}{\partial x}=0;\ \frac{\partial \vec{u}(x,0,z,t)}{\partial y}=0;\ \frac{\partial \vec{u}(x,L_y,z,t)}{\partial y}=0;$$

$$\frac{\partial \vec{u}(x,y,0,t)}{\partial z}=0;\ \frac{\partial \vec{u}(x,y,L_z,t)}{\partial z}=0;\ \vec{u}(x,y,z,0)=\vec{u}_0;\ \vec{u}(x,y,z,\infty)=\vec{u}_0.$$

We determine spatio-temporal distributions of concentrations of dopant and radiati-on defects by solving the Eqs. (1), (3) and (5) framework standard method of averaging of function corrections [28]. The method is presented in the section Appendix.

Numerical examples and discussion

In this section we analyzed dynamics of redistributions of dopant and radiation defects during annealing and under influence of mismatch-induced stress and modification of porosity. Typical distributions of concentrations of dopant in heterostructures are presented on Figs. 2 and 3 for diffusion and ion types of doping, respectively. These distributions have been calculated for the case, when value of dopant diffusion coefficient in doped area is larger, than in nearest areas. The figures show, that inhomogeneity of heterostructure gives us possibility to increase compactness of concentrations of dopants and at the same time to increase homogeneity of dopant distribution in doped part of epitaxial layer. However framework this approach of

manufacturing of bipolar transistor it is necessary to optimize annealing of dopant and/or radiation defects. Reason of this optimization is following. If annealing time is small, the dopant did not achieve any interfaces between materials of heterostructure. In this situation one cannot find any modifications of distribution of concentration of dopant. If annealing time is large, distribution of concentration of dopant is too homogenous. We optimize annealing time framework recently introduces approach [29-37]. Framework this criterion we approximate real distribution of concentration of dopant by step-wise function (see Figs. 4 and 5). Farther we determine optimal values of annealing time by minimization of the following mean-squared error.

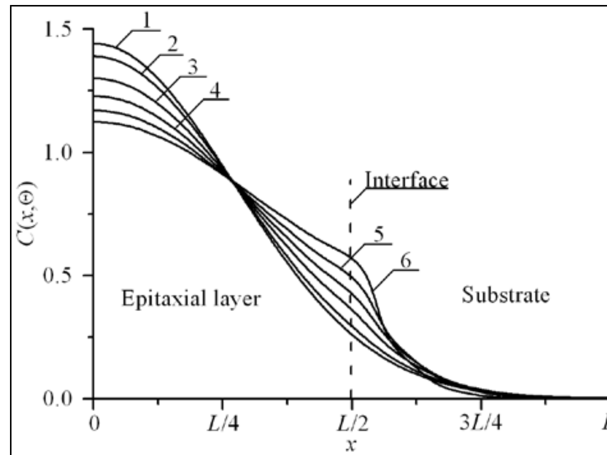

Fig 2: Distributions of concentration of infused dopant in heterostructure from Fig. 1 in direction, which is perpendicular to interface between epitaxial layer substrate. Increasing of number of curve corresponds to increasing of difference between values of dopant diffusion coefficient in layers of heterostructure under condition, when value of dopant diffusion coefficient in epitaxial layer is larger, than value of dopant diffusion coefficient in substrate

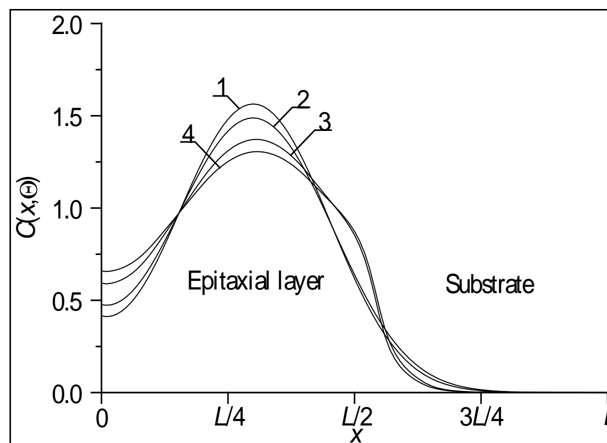

Fig 3: Distributions of concentration of implanted dopant in heterostructure from Fig. 1 in direction, which is perpendicular to interface between epitaxial layer substrate. Curves 1 and 3 corresponds to annealing time $\Theta = 0.0048(L_x^2+L_y^2+L_z^2)/D_0$. Curves 2 and 4 corresponds to annealing time $\Theta = 0.0057(L_x^2+L_y^2+L_z^2)/D_0$. Curves 1 and 2 corresponds to homogenous sample. Curves 3 and 4 corresponds to heterostructure under condition, when value of dopant diffusion coefficient in epitaxial layer is larger, than value of dopant diffusion coefficient in substrate

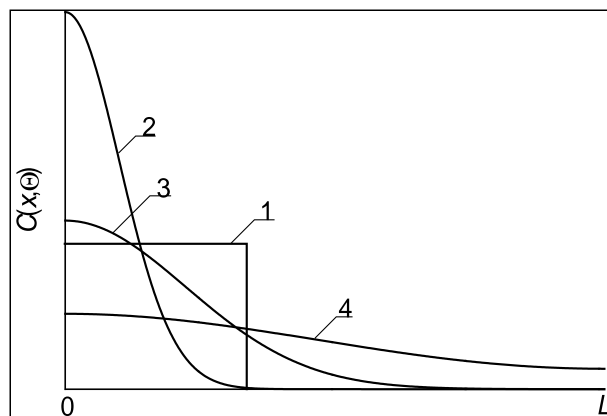

Fig 4: Spatial distributions of dopant in heterostructure after dopant infusion. Curve 1 is idealized distribution of dopant. Curves 2-4 are real distributions of dopant for different values of annealing time. Increasing of number of curve corresponds to increasing of annealing time

$$U = \frac{1}{L_x L_y L_z} \int_0^{L_x} \int_0^{L_y} \int_0^{L_z} \left[C(x,y,z,\Theta) - \psi(x,y,z) \right] d\,z\,d\,y\,d\,x, \tag{9}$$

where $\psi(x, y, z)$ is the approximation function. Dependences of optimal values of annealing time on parameters are presented on Figs. 6 and 7 for diffusion and ion types of doping, respectively. It should be noted, that it is necessary to anneal radiation defects after ion implantation. One could find spreading of concentration of distribution of dopant during this annealing. In the ideal case distribution of dopant achieves appropriate interfaces between materials of heterostructure during annealing of radiation defects. If dopant did not achieves any interfaces during annealing of radiation defects, it is practicably to additionally anneal the dopant. In this situation optimal value of additional annealing time of implanted dopant is smaller, than annealing time of infused dopant.

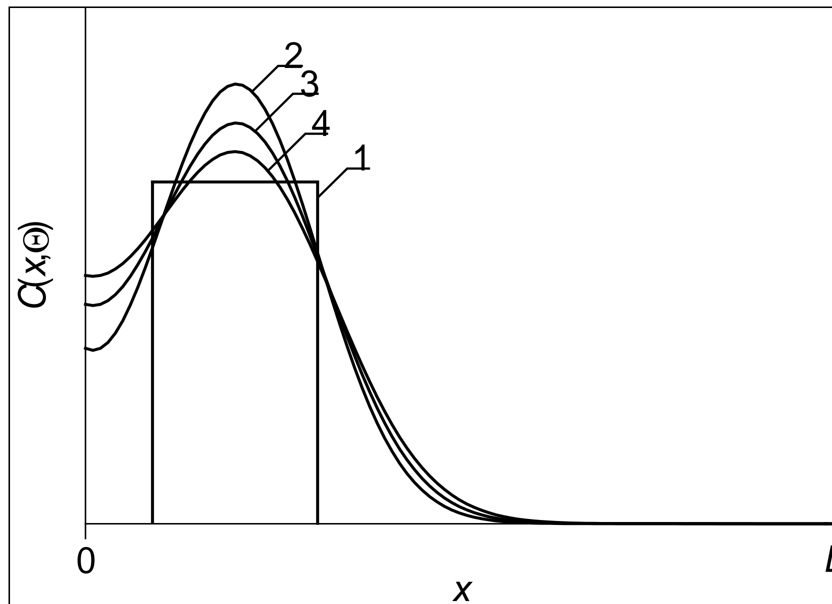

Fig 5: Spatial distributions of dopant in heterostructure after ion implantation. Curve 1 is idealized distribution of dopant. Curves 2-4 are real distributions of dopant for different values of annealing time. Increasing of number of curve corresponds to increasing of annealing time

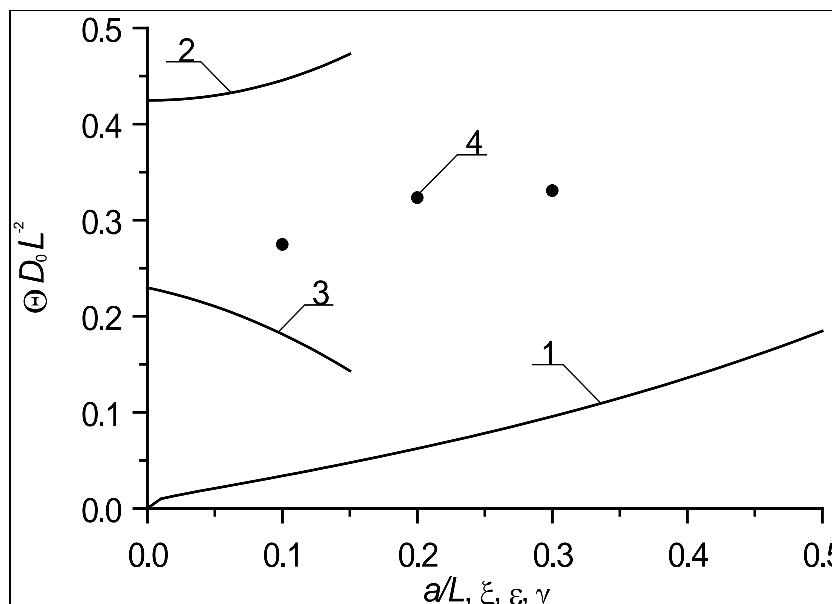

Fig 6: Dependences of dimensionless optimal annealing time for doping by diffusion, which have been obtained by minimization of mean-squared error, on several parameters. Curve 1 is the dependence of dimensionless optimal annealing time on the relation a/L and $\xi = \gamma = 0$ for equal to each other values of dopant diffusion coefficient in all parts of heterostructure. Curve 2 is the dependence of dimensionless optimal annealing time on value of parameter ε for a/L=1/2 and $\xi = \gamma = 0$. Curve 3 is the dependence of dimensionless optimal annealing time on value of parameter ξ for a/L=1/2 and $\varepsilon = \gamma = 0$. Curve 4 is the dependence of dimensionless optimal annealing time on value of parameter γ for a/L=1/2 and $\varepsilon = \xi = 0$

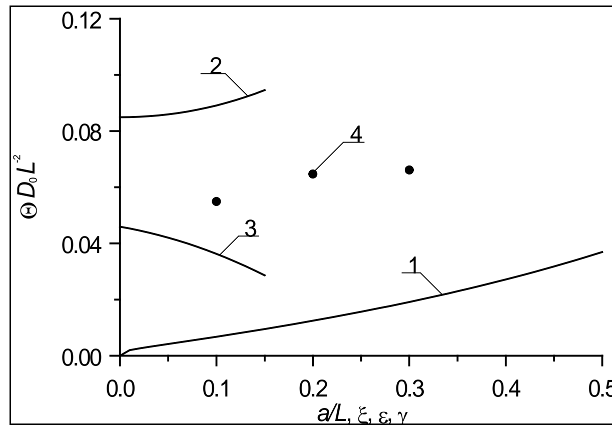

Fig 7: Dependences of dimensionless optimal annealing time for doping by ion implantation, which have been obtained by minimization of mean-squared error, on several parameters. Curve 1 is the dependence of dimensionless optimal annealing time on the relation a/L and $\xi = \gamma = 0$ for equal to each other values of dopant diffusion coefficient in all parts of heterostructure. Curve 2 is the dependence of dimensionless optimal annealing time on value of parameter ε for a/L=1/2 and $\xi = \gamma = 0$. Curve 3 is the dependence of dimensionless optimal annealing time on value of parameter ξ for a/L=1/2 and $\varepsilon = \gamma = 0$. Curve 4 is the dependence of dimensionless optimal annealing time on value of parameter γ for a/L=1/2 and $\varepsilon = \xi = 0$

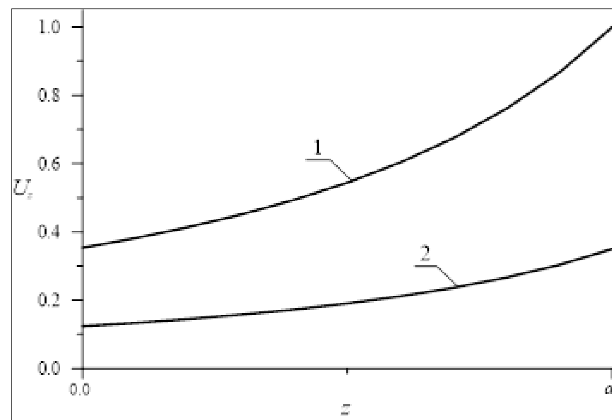

Fig 8: Normalized dependences of component u_z of displacement vector on coordinate z for nonporous (curve 1) and porous (curve 2) epitaxial layers

Table 1: dependences of optimal annealing time on several parameters for finite source of dopant

Θ	0.012	0.037	0.017	0.042	0.021	0.046
a/L	0.2	0.5	0.2	0.5	0.2	0.5
γ	1	1	2	2	3	3

Table 2: dependences of optimal annealing time on several parameters for infinite source of dopant

Θ	0.006	0.019	0.009	0.023	0.012	0.028
a/L	0.2	0.5	0.2	0.5	0.2	0.5
γ	1	1	2	2	3	3

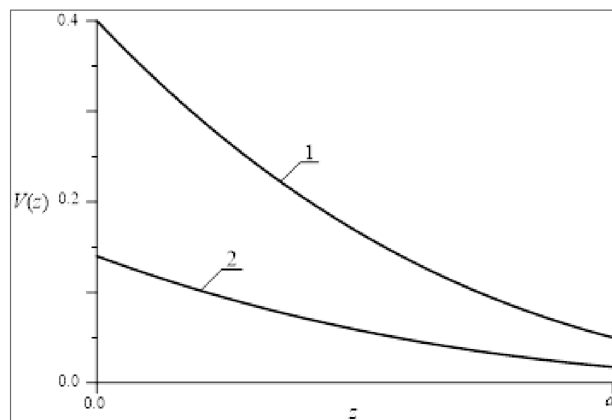

Fig 9: Normalized dependences of vacancy concentrations on coordinate z in unstressed (curve 1) and stressed (curve 2) epitaxial layers

Farther we analyzed influence of relaxation of mechanical stress on distribution of dopant in doped areas of heterostructure. Under following condition $\varepsilon_0 < 0$ one can find compression of distribution of concentration of dopant near interface between materials of heterostructure. Contrary (at $\varepsilon_0 > 0$) one can find spreading of distribution of concentration of dopant in this area. This changing of distribution of concentration of dopant could be at least partially compensated by using laser annealing [37]. This type of annealing gives us possibility to accelerate diffusion of dopant and another processes in annealed area due to in homogenous distribution of temperature and Arrhenius law. Accounting relaxation of mismatch-induced stress in heterostructure could leads to changing of optimal values of annealing time. At the same time modification of porosity gives us possibility to decrease value of mechanical stress. On the one hand mismatch-induced stress could be used to increase density of elements of integrated circuits. On the other hand could leads to generation dislocations of the discrepancy. Figs. 8 and 9 show distributions of concentration of vacancies in porous materials and component of displacement vector, which is perpendicular to interface between layers of heterostructure.

Conclusion

In this paper we analyzed redistribution of infused and implanted dopants. During the analysis it has been accounted relaxation mismatch-induced stress during manufacturing field-effect heterotransistors framework a *C*-multiplier. Based on this analysis we formulate some recommendations to optimize annealing for decreasing of dimensions of the considered transistors and for increasing their density. We also obtained some recommendations to decrease mismatch-induced stress. We introduce analytical approach for prognosis of diffusion and ion types of doping with account concurrent changing of parameters in space and time. At the same time the approach gives a possibility to take into account nonlinearity of considered processes.

References

1. Wang Z, Duan Q, Roh J. Analog. Integr. Circ. Sig. Process. 2014;81:495-501.
2. N. Ghaderi, Z.D. Ghol, S.R. Fatemi. Analog. Integr. Circ. Sig. Process. 2016;89:809-823.
3. Pushkar KL. Circuits and Systems. 2018;9(3):41-48.
4. Amhaz H, Abdallah L, Harb A, Chehadi A, Al Karim YA, Shawish A. International journal of electronic design and test. 2018;1(1):45-53.
5. Ageev AO, Belyaev AE, Boltovets NS, Ivanov VN, Konakova RV, Kudrik Ya Ya, *et al*. Sachenko. Semiconductors. 2009;43(7):897-903.
6. Jung-Hui Tsai, Shao-Yen Chiu, Wen-Shiung Lour, Der-Feng Guo. Semiconductors. 2009;43(7):971-974.
7. Chachuli SA, Fasyar PNA, Soin N, Karim NM, Yusop N. Mat. Sci. Sem. Proc. 2014;24:9-14.
8. Ermolovich IB, Milenin VV, Red'ko RA, Red'ko SM. Semiconductors. 2009;43(8):1016-1020.
9. Sinsermsuksakul P, Hartman K, Kim, J. Heo, L. Sun, H.H. Park, R. Chakraborty, T. Buonassisi, R.G. Gordon. Appl. Phys. Lett. 2013;102(5):053901-053905.
10. Reynolds JG, Reynolds Jr CL, Mohanta JF, Muth JE, Rowe HO, Everitt DE, *et al*. Phys. Lett. 2013;102(15):152114-152118.
11. Volokobinskaya NI, Komarov IN, Matyukhina TV, Reshetnikov VI, Rush AA, Falina IV, *et al*. Semiconductors. 2001;35(8):1013-1017.
12. Pankratov EL, Bulaeva EA. Reviews in Theoretical Science. 2013;1(1):58-82.
13. Kukushkin SA, Osipov AV, Romanychev AI. Physics of the Solid State. 2016;58(7):1448-1452.
14. Trukhanov EM, Kolesnikov AV, Loshkarev ID. Russian Microelectronics. 2015;44(8):552-558.
15. Pankratov EL, Bulaeva EA. Reviews in Theoretical Science. 2015;3(4):365-398.
16. Ong KK, Pey KL, Lee PS, Wee ATS, Wang XC, Chong YF. Appl. Phys. Lett. 2006;89(17):172111-172114.
17. Wang HT, Tan LS, Chor EF. J. Appl. Phys. 2006;98(9):094901-094905.
18. Yu V, Bykov AG, Yeremeev NA, Zharova IV, Plotnikov KI, Rybakov MN, *et al*. Radiophysics and Quantum Electronics. 2003;43(3):836-843.
19. Al-Absi MA, Al-Suhaibani ES, Abuelmaatti MT. Analog. Integr. Circ. Sig. Process. Vol. 90. P. 653-658 (2017).
20. Zhang YW, Bower AF. Journal of the Mechanics and Physics of Solids. 1999;47(11):2273-2297.
21. Landau LD, Lefshits EM. Theoretical physics. 7 (Theory of elasticity) Physmatlit, Moscow, 2001.
22. Kitayama M, Narushima T, Carter WC, Cannon RM, Glaeser AM. J. Am. Ceram. Soc. 2000;83:2561.
23. Kitayama M, Narushima T, Glaeser AM. J Am. Ceram. Soc. 2000;83:2572.
24. Cheremskoy PG, Slesov VV, Betekhtin VI. Pore in solid bodies Energoatomizdat, Moscow, 1990.
25. Yu Gotra Z. Technology of microelectronic devices Radio and communication, Moscow, 1991.
26. Fahey PM, Griffin PB, Plummer JD. Rev. Mod. Phys. 1989;61(2):289-388.
27. Vinetskiy VL, Kholodar GA ', Radiative physics of semiconductors. "Naukova Dumka", Kiev, 1979.
28. Mynbaeva MG, Mokhov EN, Lavrent'ev AA, Mynbaev KD. Techn. Phys. Lett. 2008;34(17):13.
29. Yu Sokolov D. Applied Mechanics. 1955;1(1):23-35.
30. Pankratov EL. Russian Microelectronics. 2007;36(1):33-39.
31. Pankratov EL. Int. J. Nanoscience. 2008;7(4-5):187-197.
32. Pankratov EL, Bulaeva EA. Reviews in Theoretical Science. 2013;1(1):58-82.
33. Pankratov EL, Bulaeva EA. Int. J. Micro-Nano Scale Transp. 2012;3(3):119-130.
34. Pankratov EL, Bulaeva EA. International Journal of Modern Physics B. 2015;29(5):1550023-1-1550023-12.
35. Pankratov EL. J. Comp. Theor. Nanoscience. 2017;14(10):4885-4899.
36. Pankratov EL, Bulaeva EA. Materials science in semiconductor processing. 2015;34:260-268.
37. Pankratov EL, Bulaeva EA. Int. J. Micro-Nano Scale Transp. 2014;4(1):17-31.
38. Pankratov EL. Nano. 2011;6(1):31-40.